Supernova neutrinos and the LSND evidence for neutrino oscillations

Michel Sorel* and Janet Conrad†
Department of Physics, Columbia University, New York, New York 10027
(Received 15 December 2001; published 23 August 2002)

The observation of the $\bar{\nu}_e$ energy spectrum from a supernova burst can provide constraints on neutrino oscillations. We derive formulas for adiabatic oscillations of supernova antineutrinos for a variety of 3- and 4-neutrino mixing schemes and mass hierarchies which are consistent with the Liquid Scintillation Neutrino Detector (LSND) evidence for $\bar{\nu}_\mu \to \bar{\nu}_e$ oscillations. Finally, we explore the constraints on these models and LSND given by the supernova SN 1987A $\bar{\nu}_e$'s observed by the Kamiokande-2 and IMB-3 detectors.

DOI: 10.1103/PhysRevD.66.033009 PACS number(s): 14.60.Pq, 14.60.St, 26.50.+x, 97.60.Bw

I. INTRODUCTION

In recent years, the treatment of neutrino transport in the environment of a core-collapse supernova (SN) explosion has improved to the point of making realistic predictions on the observables for neutrinos reaching the Earth [1–4]. Of particular interest for this paper are the average energies at the neutrinospheres, i.e. the surfaces of last scattering for the neutrinos, estimated to be 10–13 MeV for ν_e, 14–17 MeV for $\bar{\nu}_e$, 23–27 MeV for $\nu_{\mu,\tau}, \bar{\nu}_{\mu,\tau}$ [2,4].

The differences in temperatures between the various neutrino flavors can be qualitatively understood. Heavy-lepton neutrinos can interact only via neutral current (NC) processes, the main contribution to their transport opacity coming from neutrino-nucleon scattering, which dominates over neutrino-electron scattering. In addition to this same NC contribution, the transport opacity for ν_e's and $\bar{\nu}_e$'s depends also on the charged current (CC) absorptions $\nu_e + n \to p + e^-$ and $\bar{\nu}_e + p \to n + e^+$, respectively. Therefore, the ν_e- and $\bar{\nu}_e$-spheres are located at larger radii with respect to the other neutrinospheres, that is at lower densities and lower temperatures. Moreover, in a neutron-rich environment, $\nu_e + n \to p + e^-$ dominates over $\bar{\nu}_e + p \to n + e^+$: the emergent ν_e's originate from layers farther outside the center of the star compared to $\bar{\nu}_e$'s, therefore at lower temperatures. The total energy released in a SN explosion is approximately equipartitioned between the different neutrino and antineutrino flavors [3].

The above predictions can be confronted with the observation of the supernova $\bar{\nu}_e$ energy spectrum detected on Earth. Neutrino oscillations are expected to modify the spectrum since $\langle E^-_{\nu_e} \rangle < \langle E^-_{\nu_\mu, \nu_\tau} \rangle$. The energy dependence of the neutrino cross section in the detector material, approximately $\sigma^-_{\nu_e p} \propto (E^-_{\nu_e} - 1.29\ \mathrm{MeV})^2$ [5], helps in making the $\bar{\nu}_e$ energy spectrum distortion a sensitive experimental probe to neutrino oscillations. This is because higher energy neutrinos interact significantly more than lower energy ones.

We show that the extent of the spectrum modification depends crucially on the specifics of the neutrino mixing scheme and on the neutrino mass hierarchy under consideration, and we derive the relevant formulas assuming an adiabatic propagation for the antineutrinos in the supernova environment. Antineutrinos propagate adiabatically if the varying matter density they encounter changes slowly enough so that transitions between local (instantaneous) Hamiltonian eigenstates can be neglected throughout the entire antineutrino propagation. So far, neutrinos from one supernova have been detected and their energy measured: SN 1987A was observed by the Kamiokande-2 and IMB-3 detectors. The overall 20 events seen by those two detectors have all been interpreted as $\bar{\nu}_e$ interactions [6]. We examine the constraint of such observations on the LSND allowed region of $\bar{\nu}_\mu \to \bar{\nu}_e$ oscillations [7], for various neutrino mass and mixing models. If the LSND evidence is confirmed by the MiniBooNE experiment [8], several models can be excluded or constrained on the basis of the observations of the supernova SN 1987A and possibly future supernovæ.

II. ADIABATIC OSCILLATIONS AND NEUTRINO MIXING SCHEMES

A. $\bar{\nu}_e$ energy spectrum and the permutation factor

In the presence of neutrino oscillations, the $\bar{\nu}_e$ flux reaching the Earth, $F^-_{\nu_e}$, can be different from the primary flux at the neutrinosphere, $F^0_{\bar{\nu}_e}$. We will assume that, at production, the energy of active antineutrinos is equally divided into the three active flavors, i.e. that $\int_0^\infty dE^-_{\nu_\alpha} E^-_{\nu_\alpha} F^0_{\bar{\nu}_\alpha}$ has the same numerical value for $\alpha = e, \mu, \tau$. Moreover, we will also consider neutrino mixing models where the three active neutrino species are augmented by a fourth sterile neutrino with no standard weak couplings: in those cases, we will assume that the sterile component is negligible at production.

The neutrino flux reaching the Earth is

$$F^-_{\nu_e} = (p_{\mu\to e} + p_{\tau\to e}) F^0_{\bar{\nu}_\mu} + p_{e\to e} F^0_{\bar{\nu}_e}$$

$$\propto [p F^0_{\bar{\nu}_\mu} + (1-p) F^0_{\bar{\nu}_e}] \qquad (1)$$

where we have defined the *permutation factor* p as

*Electronic address: sorel@fnal.gov
†Electronic address: conrad@fnal.gov

$$p = \frac{p_{\mu\to e} + p_{\tau\to e}}{p_{\mu\to e} + p_{\tau\to e} + p_{e\to e}} \tag{2}$$

and $p_{\mu,\tau,e\to e}$ are the probabilities for a $\overline{\nu}_\mu$, $\overline{\nu}_\tau$, $\overline{\nu}_e$ respectively at the neutrinosphere to oscillate into a $\overline{\nu}_e$. In Eqs. (1), (2), we have assumed that p is energy-independent (as will be justified later), and that $\langle E_{\overline{\nu}_\mu}\rangle = \langle E_{\overline{\nu}_\tau}\rangle$. In Eq. (1), we neglect the (energy-independent) proportionality factor since we will not deal with event rates, but only with neutrino energy distributions.

B. Neutrino propagation in the adiabatic approximation

In vacuum, the Hamiltonian that governs neutrino propagation is diagonal in the mass eigenstate basis $|\nu_i\rangle$:

$$(H_0)_{ij} \equiv \langle \nu_i | H_0 | \nu_j \rangle = E_i \delta_{ij}. \tag{3}$$

If the neutrinos all have the same relativistic momentum p, their energies E_i differ only by a term proportional to their squared-mass differences, since $E_i \simeq p + m_i^2/2p$. If U is the unitary mixing matrix that relates the flavor eigenstates $|\nu_\alpha\rangle$ to the mass eigenstates via $|\nu_\alpha\rangle = U_{\alpha i}|\nu_i\rangle$, the elements of the vacuum Hamiltonian in the flavor basis are given by [9]:

$$(H_0)_{\alpha\beta} = U^*_{\alpha i} U_{\beta i} \frac{m_i^2}{2p} \tag{4}$$

where we have neglected the contribution $p\,\delta_{\alpha\beta}$ in $(H_0)_{\alpha\beta}$, which is irrelevant for neutrino oscillations.

In matter, $\overline{\nu}_e$'s undergo coherent charged current (CC) forward-scattering from electrons, and all active flavor antineutrinos coherent neutral current (NC) forward-scattering from electrons, protons, and neutrons in the medium. These processes give rise to an interaction potential $V = V_W + V_Z$, which is diagonal in the flavor basis and proportional to the matter density ρ:

$$(V)_{\alpha\beta} = A_\alpha \frac{G_F \rho}{m_N} \delta_{\alpha\beta} \tag{5}$$

where A_α is a proportionality constant, in general different for $\alpha = e$, μ, τ, or s, G_F the Fermi constant, and m_N the nucleon mass. The relevant Hamiltonian for neutrino propagation in matter is therefore $H \equiv H_0 + V$.

At the neutrinosphere, the density ρ is so high ($\sim 10^{12}$ g/cm^3 [1]) that the interaction potential dominates over the vacuum Hamiltonian, so that the propagation eigenstates coincide with the flavor eigenstates. As the propagation eigenstates free-stream outwards, toward regions of lower density, their flavor composition changes, ultimately reaching the flavor composition of the mass eigenstates in the vacuum. Given that the neutrinos escape the SN as mass eigenstates, no further flavor oscillations occur on their path to the Earth.

More specifically, making use of the adiabatic approximation and of the fact that no energy-level crossing is permitted, the flavor eigenstate at the neutrinosphere with the maximum interaction potential reaches Earth as the mass eigenstate with the biggest neutrino mass. In general, the energy level order is maintained throughout the neutrino propagation in the SN ejecta. This is illustrated in Table I for three neutrinos in the row labeled "normal $(1+1+1)$," where we have taken $A_\gamma > A_\beta > A_\alpha$ and $m_3 > m_2 > m_1$.

TABLE I. Adiabatic neutrino propagation in the SN ejecta for the neutrino mixing models considered.

Model	Hierarchy	Propagation
Normal (1+1+1)	$m_3 > m_2 > m_1$	$\overline{\nu}_\gamma \to \overline{\nu}_3$
		$\overline{\nu}_\beta \to \overline{\nu}_2$
		$\overline{\nu}_\alpha \to \overline{\nu}_1$
Normal (1+1)	$m_2 \gg m_1$	$\overline{\nu}_\mu \to \overline{\nu}_2$
		$\overline{\nu}_e \to \overline{\nu}_1$
LSND-inverted (1+1)	$m_1 \gg m_2$	$\overline{\nu}_\mu \to \overline{\nu}_1$
		$\overline{\nu}_e \to \overline{\nu}_2$
Normal (2+1)	$m_3 > m_2 \gg m_1$	$\overline{\nu}_\mu \to \overline{\nu}_3$
		$\overline{\nu}_\tau \to \overline{\nu}_2$
		$\overline{\nu}_e \to \overline{\nu}_1$
LSND-inverted (2+1)	$m_1 \gg m_3 > m_2$	$\overline{\nu}_\mu \to \overline{\nu}_1$
		$\overline{\nu}_\tau \to \overline{\nu}_3$
		$\overline{\nu}_e \to \overline{\nu}_2$
Normal (2+2)	$m_3 > m_2 \gg m_1 > m_0$	$\overline{\nu}_\mu \to \overline{\nu}_3$
		$\overline{\nu}_\tau \to \overline{\nu}_2$
		$\overline{\nu}_s \to \overline{\nu}_1$
		$\overline{\nu}_e \to \overline{\nu}_0$
LSND-inverted (2+2)	$m_1 > m_0 \gg m_3 > m_2$	$\overline{\nu}_\mu \to \overline{\nu}_1$
		$\overline{\nu}_\tau \to \overline{\nu}_0$
		$\overline{\nu}_s \to \overline{\nu}_3$
		$\overline{\nu}_e \to \overline{\nu}_2$
Normal (3+1)	$m_4 \gg m_3 > m_2 > m_1$	$\overline{\nu}_\mu \to \overline{\nu}_4$
		$\overline{\nu}_\tau \to \overline{\nu}_3$
		$\overline{\nu}_s \to \overline{\nu}_2$
		$\overline{\nu}_e \to \overline{\nu}_1$
LSND-inverted (3+1)	$m_3 > m_2 > m_1 \gg m_4$	$\overline{\nu}_\mu \to \overline{\nu}_3$
		$\overline{\nu}_\tau \to \overline{\nu}_2$
		$\overline{\nu}_s \to \overline{\nu}_1$
		$\overline{\nu}_e \to \overline{\nu}_4$

For example, the probability for a $\overline{\nu}_\alpha$ to emerge from the SN environment as a $\overline{\nu}_\beta$ is given by

$$\begin{aligned} p_{\alpha\to\beta} &= |\langle \overline{\nu}_\beta | U^{evol} | \overline{\nu}_\alpha \rangle|^2 = |\langle U_{\beta i} \overline{\nu}_i | U^{evol} | \overline{\nu}_\alpha \rangle|^2 \\ &= |U^*_{\beta i} \delta_{i,1}|^2 = |U_{\beta 1}|^2 \end{aligned} \tag{6}$$

where U^{evol} is the adiabatic evolution operator. In Eq. (6), we have used Table I to get

$$\langle \overline{\nu}_i | U^{evol} | \overline{\nu}_\alpha \rangle = \delta_{i,1}. \tag{7}$$

TABLE II. Results on the probabilities $p_{\mu,\tau,e\to e}$ for a $\overline{\nu}_{\mu,\tau,e}$ to emerge from the SN as a $\overline{\nu}_e$, the permutation factor p of Eq. 2, and the LSND oscillation amplitude $\sin^2 2\vartheta_{LSND}$, for the various neutrino mixing schemes considered.

Model	Mixing	$p_{\mu\to e}$	$p_{\tau\to e}$	$p_{e\to e}$	p	$\sin^2 2\vartheta_{LSND}$
Normal (1+1)	Eq. (10)	$\sin^2\vartheta$	0	$\cos^2\vartheta$	$\sin^2\vartheta$	$\sin^2 2\vartheta = 4p(1-p)$
LSND-inverted (1+1)	Eq. (10)	$\cos^2\vartheta$	0	$\sin^2\vartheta$	$\cos^2\vartheta$	$\sin^2 2\vartheta = 4p(1-p)$
Normal (2+1)	Eq. (11)	$\frac{3}{4}\alpha^2$	$\frac{1}{4}\alpha^2$	1	$\alpha^2/(1+\alpha^2)$	$4\alpha^2 = 4p/(1-p)$
LSND-inverted (2+1)	Eq. (11)	1	$\frac{3}{4}\alpha^2$	$\frac{1}{4}\alpha^2$	$(1+\frac{3}{4}\alpha^2)/(1+\alpha^2)$	$4\alpha^2 = 4(1-p)/(p-\frac{3}{4})$
Normal (2+2)	Eq. (14)	β^2	β^2	$\frac{1}{2}$	$4\beta^2/(1+4\beta^2)$	$8\beta^2 = 2p/(1-p)$
LSND-inverted (2+2)	Eq. (14)	$\frac{1}{2}$	$\frac{1}{2}$	β^2	$1/(1+\beta^2)$	$8\beta^2 = 8(1-p)/p$
Normal (3+1)	Eq. (15)	γ^2	0	$\frac{1}{2}$	$2\gamma^2/(1+2\gamma^2)$	$4\gamma^2\delta^2 = 2\delta^2 p/(1-p)$
LSND-inverted (3+1)	Eq. (15)	0	$\frac{1}{2}$	γ^2	$1/(1+2\gamma^2)$	$4\gamma^2\delta^2 = 2\delta^2(1-p)/p$

This result can be immediately generalized to any number of antineutrino generations. Also, as long as the adiabatic approximation is satisfied, the formula does not depend on the specific dynamics for the neutrino propagation, for example on the number and position in the SN environment of Mikheyev-Smirnov-Wolfenstein (MSW) resonances. We will comment more on the validity of the adiabatic approximation in the next section.

In this paper, we consider three or four flavor components, including a sterile one. At tree-level, the proportionality factors A_α in the interaction potential for neutral matter are [9,10]

$$A = \begin{cases} (1-3Y_e)/\sqrt{2} & \text{for} \quad \overline{\nu}_e, \\ (1-Y_e)/\sqrt{2} & \text{for} \quad \overline{\nu}_\mu, \overline{\nu}_\tau, \\ 0 & \text{for} \quad \overline{\nu}_s, \end{cases} \tag{8}$$

where Y_e is the electron fraction per nucleon. Following the assumptions of [10,11], we use $Y_e \simeq (1+\langle E^-_{\nu_e}\rangle/\langle E_{\nu_e}\rangle)^{-1} > 1/3$ at the neutrinosphere. Considering also one-loop electroweak radiative corrections, a difference in the $\overline{\nu}_\mu$ and $\overline{\nu}_\tau$ interaction potentials of magnitude $(A_\mu - A_\tau)/A_\mu \sim 10^{-4}$ appears due to the difference in the charged lepton masses [12,13]. At the neutrinosphere, this second-order effect in the interaction potential dominates over the vacuum Hamiltonian terms (as long as $|m_i^2 - m_j^2| < 10$ eV^2 for all i,j), and removes the $\overline{\nu}_\mu - \overline{\nu}_\tau$ degeneracy. Therefore, for the antineutrino channel considered here, we take

$$A_\mu > A_\tau > A_s > A_e . \tag{9}$$

For the neutrino channel, one should substitute $A \to -A$ in Eq. (8), and the order in Eq. (9) would be inverted.

Therefore, given a specific neutrino mass and mixing model, the permutation factor can be easily evaluated in the adiabatic approximation, and its numerical value does not depend on the neutrino energy. We will comment on possible energy-dependent Earth matter effects in the next section. In practice, one proceeds backwards: given a certain measured value of p, it is possible to constrain possible models for neutrino oscillations. This approach is used for example in [13] to constrain models explaining the solar and atmospheric neutrino data; in this paper, we focus on 3 and 4-neutrino models explaining the Liquid Scintillation Neutrino Detector (LSND) data.

C. Possible mixing schemes

The results for the $\overline{\nu}_\mu$, $\overline{\nu}_\tau$, $\overline{\nu}_e \to \overline{\nu}_e$ adiabatic oscillation probabilities, the permutation factor p, and the LSND oscillation amplitude $\sin^2 2\vartheta$ as a function of the mixing parameters and p for the eight possible mass and mixing schemes considered below are given in Table II. The mass hierarchy and the adiabatic propagation of the neutrino eigenstates for these mixing schemes are depicted in Table I.

The simplest possible mixing scheme is a (1+1) model explaining only $\overline{\nu}_\mu \to \overline{\nu}_e$ LSND oscillations in vacuum, and not the atmospheric or solar oscillations:

$$\begin{pmatrix} \overline{\nu}_e \\ \overline{\nu}_\mu \end{pmatrix} = \begin{pmatrix} \cos\vartheta & \sin\vartheta \\ -\sin\vartheta & \cos\vartheta \end{pmatrix} \begin{pmatrix} \overline{\nu}_1 \\ \overline{\nu}_2 \end{pmatrix}, \tag{10}$$

where the mixing angle ϑ can assume any value in the range $0 < \vartheta < \pi/4$.

We consider a (2+1) model motivated, for example, by CPT-violating scenarios (see, e.g. [14]), in which atmospheric and LSND oscillations in the antineutrino channel are obtained via the mixing [15]:

$$\begin{pmatrix} \overline{\nu}_e \\ \overline{\nu}_\mu \\ \overline{\nu}_\tau \end{pmatrix} = \begin{pmatrix} 1 & -\frac{1}{2}\alpha & -\frac{\sqrt{3}}{2}\alpha \\ \alpha & \frac{1}{2} & \frac{\sqrt{3}}{2} \\ 0 & -\frac{\sqrt{3}}{2} & \frac{1}{2} \end{pmatrix} \begin{pmatrix} \overline{\nu}_1 \\ \overline{\nu}_2 \\ \overline{\nu}_3 \end{pmatrix}. \tag{11}$$

The matrix in Eq. (11) is chosen to ensure large $\overline{\nu}_\mu \to \overline{\nu}_\tau$ mixing for atmospheric neutrinos ($\sin^2 2\vartheta_{atm} = 3/4$), while the LSND $\overline{\nu}_\mu \to \overline{\nu}_e$ mixing is fixed by the parameter α ($\sin^2 2\vartheta_{LSND} = 4\alpha^2$).

The most popular models which explain the solar, atmospheric and LSND signatures (and the null results obtained

by other experiments) via neutrino oscillations invoke the existence of a sterile neutrino $\overline{\nu}_s$. One example of a (2+2) model is the following, which is taken from [16]:

$$\begin{pmatrix} \overline{\nu}_s \\ \overline{\nu}_e \\ \overline{\nu}_\mu \\ \overline{\nu}_\tau \end{pmatrix} = \begin{pmatrix} \frac{1}{\sqrt{2}} & \frac{1}{\sqrt{2}} & 0 & 0 \\ -\frac{1}{\sqrt{2}} & \frac{1}{\sqrt{2}} & \beta & \beta \\ \beta & -\beta & \frac{1}{\sqrt{2}} & \frac{1}{\sqrt{2}} \\ 0 & 0 & -\frac{1}{\sqrt{2}} & \frac{1}{\sqrt{2}} \end{pmatrix} \begin{pmatrix} \overline{\nu}_0 \\ \overline{\nu}_1 \\ \overline{\nu}_2 \\ \overline{\nu}_3 \end{pmatrix} \tag{12}$$

where one pair of nearly degenerate mass eigenstates has maximal $\nu_e \to \nu_s$ mixing for solar neutrinos and the other pair has maximal $\nu_\mu \to \nu_\tau$ mixing for atmospheric neutrinos. Small inter-doublet mixings through the β parameter accommodate the LSND result ($\sin^2 2\vartheta_{LSND} = 8\beta^2$).

Recent experimental results [17] show that pure $\nu_e \to \nu_s$ solar oscillations are excluded at high significance. We therefore consider a more general (2+2) scenario, in which solar neutrinos can undergo any combination of $\nu_e \to \nu_s$ and $\nu_e \to \nu_\tau$ oscillations, while atmospheric neutrinos can undergo any combination of $\nu_\mu \to \nu_\tau$ and $\nu_\mu \to \nu_s$ oscillations. We follow the procedure in [18] to obtain this more general mixing starting from Eq. (12), by substituting the $(\overline{\nu}_s, \overline{\nu}_\tau)$ states with the rotated states $(\overline{\nu}'_s, \overline{\nu}'_\tau)$:

$$\begin{pmatrix} \overline{\nu}'_s \\ \overline{\nu}'_\tau \end{pmatrix} = \begin{pmatrix} \cos\varphi_s & \sin\varphi_s \\ -\sin\varphi_s & \cos\varphi_s \end{pmatrix} \begin{pmatrix} \overline{\nu}_s \\ \overline{\nu}_\tau \end{pmatrix} \tag{13}$$

where the rotation angle φ_s fixes the sterile component in the atmospheric doublet ($0 < \varphi_s < \pi/2$). Equation (12) then becomes

$$\begin{pmatrix} \overline{\nu}_s \\ \overline{\nu}_e \\ \overline{\nu}_\mu \\ \overline{\nu}_\tau \end{pmatrix} = \begin{pmatrix} \frac{\cos\varphi_s}{\sqrt{2}} & \frac{\cos\varphi_s}{\sqrt{2}} & \frac{\sin\varphi_s}{\sqrt{2}} & -\frac{\sin\varphi_s}{\sqrt{2}} \\ -\frac{1}{\sqrt{2}} & \frac{1}{\sqrt{2}} & \beta & \beta \\ \beta & -\beta & \frac{1}{\sqrt{2}} & \frac{1}{\sqrt{2}} \\ \frac{\sin\varphi_s}{\sqrt{2}} & \frac{\sin\varphi_s}{\sqrt{2}} & -\frac{\cos\varphi_s}{\sqrt{2}} & \frac{\cos\varphi_s}{\sqrt{2}} \end{pmatrix} \begin{pmatrix} \overline{\nu}_0 \\ \overline{\nu}_1 \\ \overline{\nu}_2 \\ \overline{\nu}_3 \end{pmatrix} \tag{14}$$

which contains Eq. (12) in the specific case $\varphi_s = 0$. We note that the LSND oscillation amplitude formula $\sin^2 2\vartheta_{LSND} = 8\beta^2$ holds also for the more general case of Eq. (14), and that our results are independent of the value of φ_s (see Table II).

Another possible 4-neutrino model has a (3+1) hierarchy; as an example for this model, here we consider the following mixing, which is also taken from [16]:

$$\begin{pmatrix} \overline{\nu}_e \\ \overline{\nu}_\mu \\ \overline{\nu}_\tau \\ \overline{\nu}_s \end{pmatrix} = \begin{pmatrix} \frac{1}{\sqrt{2}} & \frac{1}{\sqrt{2}} & 0 & \gamma \\ -\frac{1}{2} & \frac{1}{2} & \frac{1}{\sqrt{2}} & \delta \\ \frac{1}{2} & -\frac{1}{2} & \frac{1}{\sqrt{2}} & 0 \\ \frac{1}{2}\delta - \frac{1}{\sqrt{2}}\gamma & -\frac{1}{2}\delta - \frac{1}{\sqrt{2}}\gamma & -\frac{1}{\sqrt{2}}\delta & 1 \end{pmatrix} \times \begin{pmatrix} \overline{\nu}_1 \\ \overline{\nu}_2 \\ \overline{\nu}_3 \\ \overline{\nu}_4 \end{pmatrix} \tag{15}$$

where the solar and atmospheric oscillations are approximately described by oscillations of three active neutrinos, and the LSND result by a coupling of $\overline{\nu}_\mu$ and $\overline{\nu}_e$ through small mixings with $\overline{\nu}_s$ that has a mass eigenvalue widely separated from the others ($\sin^2 2\vartheta_{LSND} = 4\gamma^2\delta^2$). For the (3+1) scenario, the constraint given by the permutation probability p is not sufficient to determine the LSND oscillation amplitude $\sin^2 2\vartheta_{LSND}$. Therefore, the constraint on $|U_{\mu 4}|^2 = \delta^2$ given by the CDHS and Super-K experiments will also be used, as explained later.

We should note that the mixing matrices defined in Eqs. (10)–(15) are approximations in the sense that the matrices are unitary only up to order $\mathcal{O}(\alpha, \beta, \gamma, \delta)$. These are the parameters in the mixings responsible for LSND-type oscillations, which we let float for our analysis, but we know they are small.

In order to determine the permutation factor for the mixing models, we also need to specify the neutrino mass hierarchy. In this paper, we consider for each mixing model both the cases of "normal" and "LSND-inverted" mass hierarchies. By "normal" hierarchy, here we mean that $m_i > m_j$ for $i > j$, where m_i is the mass eigenvalue for the $|\overline{\nu}_i\rangle$ state. We define the "LSND-inverted" hierarchies as the ones obtained substituting $\Delta m_{LSND} \to -\Delta m_{LSND}$ in the normal hierarchies, without changing the hierarchy of the eventual solar and atmospheric splittings (see Table I); Δm_{LSND} is the neutrino mass difference responsible for LSND oscillations.

A common feature to all the mixing schemes is apparent in Table II. In the adiabatic approximation, normal mass hierarchies predict small permutation factors, while an almost complete permutation would be present for LSND-inverted hierarchies.

Given the specific neutrino mixing models considered here, we can now partially address the question whether the adiabatic approximation is applicable in this context. At a

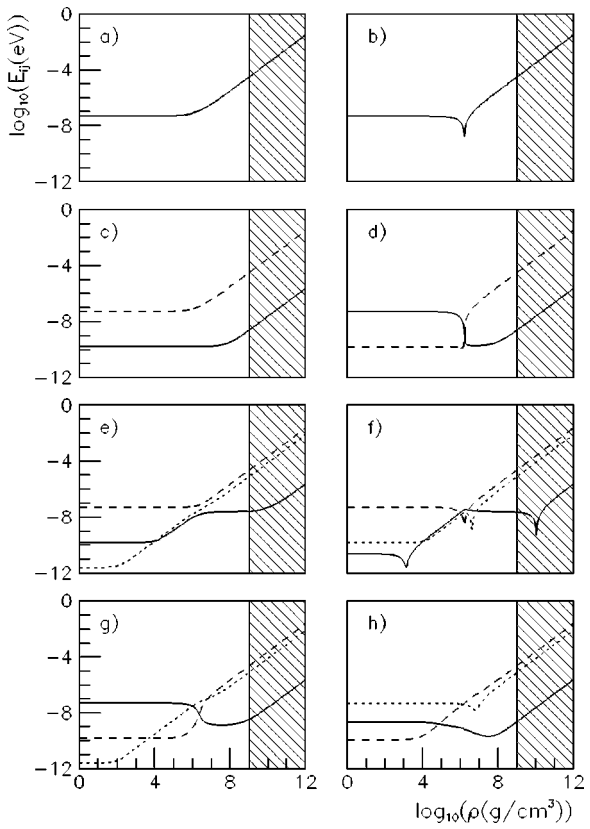

FIG. 1. Splittings between energy eigenvalues versus matter density ρ for various neutrino mass and mixing models. Solid, dashed, dotted lines show the splittings E_{12}, E_{23}, E_{34}, respectively (see text). The local minima correspond to MSW-resonances. Model (a) normal (1+1); (b) inverted (1+1); (c) normal (2+1); (d) inverted (2+1); (e) normal (2+2); (f) inverted (2+2); (g) normal (3+1); (h) inverted (3+1). Apart from the inconsequential $\overline{\nu}_\mu \leftrightarrow \overline{\nu}_\tau$ one in (f), no MSW-resonances occur before the antineutrinos reach the stalled shock-wave (hatched area).

resonance, where the nonadiabaticity is maximal, this is a good approximation if the width of the resonance region is large compared with the local neutrino oscillation length. The width of the resonance is, in turn, determined by the characteristic length scale of the radial matter density variations at the resonance. While there are reliable models for the matter density profile of the progenitor star, there are still uncertainties on the profile seen by neutrinos in their free-streaming propagation.

It is now thought that neutrino heating of the proto-neutron star mantle drives the supernova explosion, which would happen with a ~ 1 s delay after the creation of the shock-wave, ultimately responsible for the explosion; during this delay, the shock-wave would be stalled at a radius of ~ 200 km from the neutron star, corresponding to a density $\rho \sim 10^9 - 10^{10}$ g/cm^3 [1]. Therefore, the density profile in the proximity of the stalled shock-wave, which is difficult to model reliably, is a potential site for nonadiabatic oscillations.

In Fig. 1 we show the energy splittings between the local neutrino energy eigenvalues E_i, as a function of matter density, for all eight neutrino models considered here. For an n-neutrino model, we plot $E_{i,i+1} \equiv E_i - E_{i+1}$, where $i = 1, \ldots, n-1$; the eigenvalues are ordered such that $E_1 > E_2 > \ldots > E_n$. Clearly, a resonance corresponds to a local minimum in one of the curves. As can be seen from Fig. 1, all the resonances [except the inconsequential one in Fig. 1(f) between $\overline{\nu}_\mu$ and $\overline{\nu}_\tau$ [19]] lie at densities well below the stalled shock-wave density of $\rho \sim 10^9 - 10^{10}$ g/cm^3. Therefore, the impact of level crossing between propagation eigenstates is likely to be small even where the neutrinos encounter the shock-wave.

If the SN neutrinos cross the Earth on their way to the detector, as for example happened for the SN 1987A $\overline{\nu}_e$'s detected by the Kamiokande-2 and IMB-3 detectors, it is also necessary to evaluate the importance of Earth matter effects in the neutrino propagation. Clearly, for neutrino oscillation models where no solar splitting is involved [for example the (1+1) and (2+1) models in this paper], this effect is negligible. In the models where such a splitting is allowed [i.e. the (2+2) and (3+1) models considered here], the situation is more complicated. However, the Earth matter effects have been shown to be small in this case as well for a large fraction of the SN $\overline{\nu}_e$ energy spectrum (below $\simeq 40$ MeV) [13,20], and for the sake of simplicity will not be considered further.

III. CONSTRAINTS ON LSND FROM SN 1987A OBSERVATIONS

Twenty $\overline{\nu}_e$ events from the supernova SN 1987A were observed by the Kamiokande-2 (Kam-2) and IMB-3 detectors. Kam-2 saw 12 events with an average energy of $\langle E_{det} \rangle = 14.7$ MeV, IMB-3 (which had a higher energy threshold than Kam-2) detected 8 events with $\langle E_{det} \rangle = 31.9$ MeV [21].

From a comparison of the measured energy spectra ($F_{\overline{\nu}_e}$) with theoretical models of neutrino emission ($F^0_{\nu_e}$ and $F^0_{\nu_\mu}$), it is possible to infer the permutation factor p in Eq. (1). SN 1987A observations are consistent with no-oscillations (i.e. $p=0$). In Appendix A, we derive a conservative upper bound on p of $p<0.22$ at 99% C.L., by applying a Kholmogorov-Smirnov test on the joint Kam-IMB dataset and a range of supernova neutrino emission models.

One important result of our analysis is immediately apparent from the values of the permutation factors p as a function of the mixing parameters in Table II, and from the fact that the value of p inferred from SN 1987A data has to be less than 0.22 at 99% C.L. The four mixing schemes considered, explaining the LSND effect via a LSND-inverted neutrino mass hierarchy, are all incompatible with SN 1987A data.

We now consider the normal hierarchy cases. For the (1+1), (2+1) and (2+2) models with the mixings of Eqs. (10)–(12), the bound on the permutation factor p unambiguously determines the constraint on the LSND oscillation amplitude $\sin^2 2\vartheta_{LSND}$ (see Table II). At 99% C.L., SN 1987A data provide no constraints on the (2+1) model, and a constraint which is weaker than existing bounds from the accel-

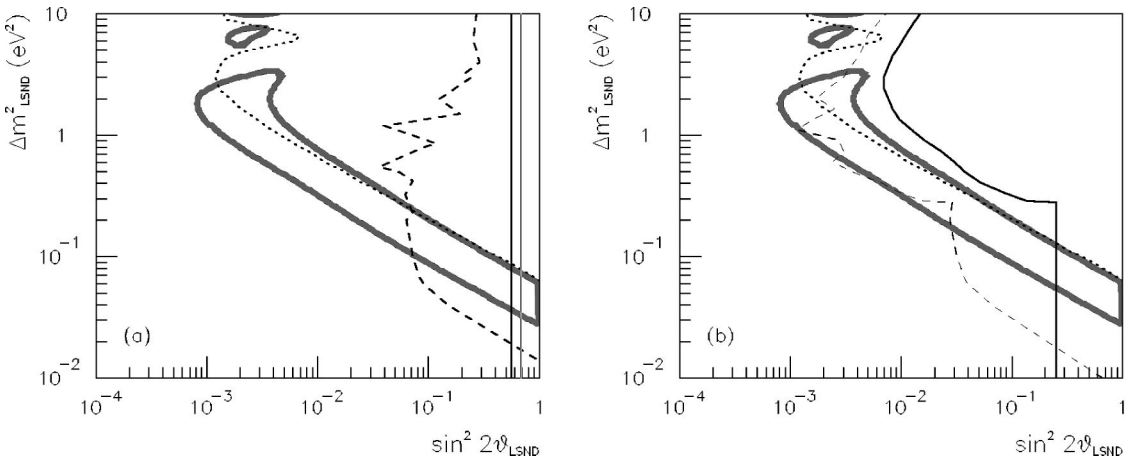

FIG. 2. 99% C.L. LSND allowed region [7] and 99% C.L. exclusion regions for the neutrino mixing schemes considered in the text and with normal mass hierarchy. The exclusion regions are estimated as in [26]. (a) shows the exclusion regions for the $(1+1)$, $(2+1)$ and $(2+2)$ models, (b) for the $(3+1)$ model. The exclusion regions refer to experimental data from the following experiments. (a) Dotted line: KARMEN; dashed line: Bugey; dark solid line: SN 1987A for the $(2+2)$ model; light solid line: SN 1987 for the $(1+1)$ model; SN 1987A data provide no constraints at 99% C.L. for the $(2+1)$ model. (b) Dotted line: KARMEN; dashed line: Bugey, CDHS and Super-K; solid line: SN 1987A, CDHS and Super-K.

erator experiment KARMEN [23] and the reactor experiment Bugey [24,25] for the $(1+1)$ and $(2+2)$ models [see Fig. 2(a)]. Therefore, these models are compatible with the SN 1987A data.

As already mentioned, for the $(3+1)$ model, the permutation factor does not fully determine the LSND oscillation amplitude: $\sin^2 2\vartheta_{LSND}$ depends not only on p, but also on $|U_{\mu 4}|^2=\delta^2$. Here we use the Δm^2_{LSND}-dependent constraints on δ^2 from the ν_μ-disappearance experiments CDHS (for $\Delta m^2_{LSND}>0.3$ eV^2) and Super-K (for $\Delta m^2_{LSND}<0.3$ eV^2) [25]. Moreover, another complication arises in evaluating exclusion regions for $(3+1)$ models: given the 99% C.L. upper bounds on $\gamma^2=|U_{e4}|^2$ from SN 1987A and $\delta^2=|U^2_{\mu 4}|$ from CDHS and Super-K, what is the 99% C.L. upper bound on $\sin^2 2\vartheta_{LSND}=4\gamma^2\delta^2$? We follow the method described in [26] to estimate this bound. The same method is applied to estimate the 99% C.L. upper limit on $\sin^2 2\vartheta_{LSND}$ coming from Bugey (for γ^2) and CDHS and Super-K (for δ^2), that is without using the SN 1987A data. The results for the $(3+1)$ model with normal neutrino mass hierarchy and mixing given by Eq. (15) are shown in Fig. 2(b). Also for this model, we find that existing constraints (the Bugey constraint on δ^2, in this case) are stronger than the SN 1987A one.

Table III summarizes the SN 1987A constraints obtained in this paper on the LSND allowed region, for the various neutrino mass and mixing models considered.

IV. CONCLUSIONS

We have investigated the effect that 3- and 4-neutrino oscillation schemes would have in modifying the energy spectrum of supernova $\bar{\nu}_e$'s. Throughout the paper, we apply the adiabatic approximation for the antineutrino propagation in the supernova environment and neglect Earth matter effects. Moreover, we have used our results to test the compatibility between the SN 1987A data and the LSND evidence for $\bar{\nu}_\mu \to \bar{\nu}_e$ oscillations.

We have provided specific relations for the permutation factor, which gives the admixture of a higher energy flux to the original $\bar{\nu}_e$ flux at production from $\bar{\nu}_\mu, \bar{\nu}_\tau \to \bar{\nu}_e$ oscillations, for various neutrino mass and mixing models. The permutation factor may be measurable with good accuracy in future supernova experiments.

Based on SN 1987A data only, which seem to indicate a small (if nonzero) value for the permutation factor, we are able to exclude all of the four models considered which would explain the LSND signal via a ''LSND-inverted'' neutrino mass hierarchy, as defined in the text. For the normal mass hierarchy schemes considered, SN 1987A data do not provide any stronger constraints on the LSND allowed region for oscillations than those already obtained with reactor, accelerator and atmospheric neutrinos; additional experimental input is necessary to unambiguously discern the neutrino mass and mixing properties. Undoubtedly, the detection of

TABLE III. Summary of the SN 1987A constraints on the LSND allowed region, for the various models considered in this paper; see Fig. 2 also.

Model	SN 1987A constraint on LSND region (99% C.L.)
Normal $(1+1)$	partially excluded [Fig. 2(a)]
LSND-inverted $(1+1)$	excluded
Normal $(2+1)$	unconstrained
LSND-inverted $(2+1)$	excluded
Normal $(2+2)$	partially excluded [Fig. 2(a)]
LSND-inverted $(2+2)$	excluded
Normal $(3+1)$	partially excluded [Fig. 2(b)]
LSND-inverted $(3+1)$	excluded

supernova neutrinos by present or near-term experiments [27] would prove very useful in this respect.

ACKNOWLEDGMENTS

We thank Kevork Abazajian, Vernon Barger, John Beacom, Nicole Bell, Steve Brice, Klaus Eitel, Lam Hui, Hitoshi Murayama and Michael Shaevitz for valuable discussions and useful suggestions. This work was supported by NSF and by the Sloan Foundation.

APPENDIX: UPPER BOUNDS ON THE PERMUTATION FACTOR FROM SN 1987A DATA

In this appendix, we discuss the statistical methodology and the physics assumptions used to estimate the upper bound on the permutation factor p quoted in the text, $p<0.22$ at 99% C.L. We use the same statistical methodology as in [22], that is we use the Kholmogorov-Smirnov test on the joint Kam-IMB dataset to derive the upper bound. Most of the physics assumptions are identical to those in [28].

The expected energy spectrum for the positrons, observed in the Kamiokande and IMB detectors via the reaction $\bar{\nu}_e p \rightarrow e^+ n$, is

$$n_i(E_{det}) = \frac{N_{p,i}}{4\pi D^2}\int_0^\infty dE_+ P_i(E_{det},E_+) \times \eta_{0,i}(E_+)\sigma^-_{\nu_e p}(E_+ + Q)F^-_{\nu_e}(E_+ + Q) \tag{A1}$$

where i refers to either Kam or IMB, $N_{p,i}$ is the number of target protons in the detectors, D the distance between the Large Magellanic Cloud and the Earth, E_{det} (E_+) is the detected (true) positron energy, $Q \equiv m_n - m_p = 1.29$ MeV$\simeq E^-_{\nu_e} - E_+$, $P_i(E_{det},E_+)$, and $\eta_{0,i}(E_+)$ the energy resolution functions and efficiency curves taken from [28], $\sigma^-_{\nu_e p}(E_+ + Q) \propto E_+^2$ the neutrino interaction cross section taken from [5] (neglecting nuclear recoil), and finally $F^-_{\nu_e}(E_+ + Q)$ the neutrino flux at the detector taken from Eq. (1). We assume "unpinched" Fermi-Dirac distributions for the fluxes $F^0_{\nu_\alpha}$, $\alpha = e,\mu$, appearing in Eq. (1):

$$F^0_{\nu_\alpha}(E) \propto \frac{E^2}{\langle E^-_{\nu_\alpha}\rangle T_\alpha^3 (e^{E/T_\alpha}+1)} \tag{A2}$$

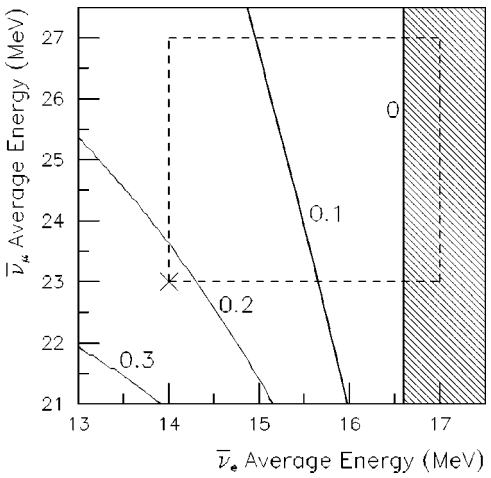

FIG. 3. Solid lines: isocontours for the *upper bounds* on the permutation factor p at 99% C.L. obtained from SN 1987A data, as a function of the $\bar{\nu}_e$ and $\bar{\nu}_\mu$ average energies predicted at production by supernova models; rectangle with dashed border: range of energies allowed by present models; cross: model chosen to derive the (conservative) upper bound on p used in the text. The region $\langle E^-_{\nu_e}\rangle > 16.6$ MeV is excluded at 99% C.L. for all values of p.

where $\langle E^-_{\nu_\alpha}\rangle \simeq 3.15 T_\alpha$ at the denominator ensures energy equipartition.

The cumulative distribution function used for the Kholmogorov-Smirnov test is

$$\mathcal{F}(E_{det}) = \int_0^{E_{det}} dE[n_{Kam}(E) + n_{IMB}(E)]. \tag{A3}$$

Figure 3 shows the upper bound on the permutation factor p obtained from SN 1987A data, at 99% C.L., as a function of the average energies $\langle E^-_{\nu_e}\rangle$, $\langle E^-_{\nu_\mu}\rangle$. As expected, the bound becomes more stringent for supernova models in which the neutrino average energies are higher. SN 1987A data are incompatible at 99% C.L. with all supernova neutrino models predicting $\langle E^-_{\nu_e}\rangle > 16.6$ MeV, for all values of p and $\langle E^-_{\nu_\mu}\rangle$. We adopt a conservative approach, and quote as the upper bound on p the largest value for supernova neutrino models in the range $14 < \langle E^-_{\nu_e}\rangle < 17$ MeV, $23 < \langle E^-_{\nu_\mu}\rangle < 27$ MeV, that is the one corresponding to $\langle E^-_{\nu_e}\rangle = 14$ MeV, $\langle E^-_{\nu_\mu}\rangle = 23$ MeV (cross in Fig. 3).

[1] A. Burrows *et al.*, Astrophys. J. **539**, 865 (2000).

[2] H.-T. Janka, in Proceedings of the Vulcano Workshop 1992, Frontier objects in astrophysics and particle physics, pp. 345–374.

[3] H.-T. Janka, Astropart. Phys. **3**, 377 (1995).

[4] G.G. Raffelt, Nucl. Phys. B (Proc. Suppl.) **110**, 254 (2002).

[5] P. Vogel and J.F. Beacom, Phys. Rev. D **60**, 053003 (1999).

[6] There has been some discussion whether to interpret the first Kam-2 event as $\bar{\nu}_e$ or ν_e, see for example H. Murayama and T. Yanagida, Phys. Lett. B **520**, 263 (2001). The Kam-2 Collaboration prefers to interpret all their 12 events as $\bar{\nu}_e$ interactions; see [21] for a discussion.

[7] LSND Collaboration, A. Aguilar *et al.*, Phys. Rev. D **64**, 112007 (2001).

[8] MiniBooNE Collaboration, A. Bazarko, Nucl. Phys. B (Proc. Suppl.) **91**, 210 (2000).

[9] B. Kayser, hep-ph/0104147.
[10] D.O. Caldwell, G.M. Fuller, and Y.Z. Qian, Phys. Rev. D **61**, 123005 (2000).
[11] Y.Z. Qian *et al.*, Phys. Rev. Lett. **71**, 1965 (1993).
[12] F.J. Botella, C.S. Lim, and W.J. Marciano, Phys. Rev. D **35**, 896 (1987).
[13] A.S. Dighe and A.Y. Smirnov, Phys. Rev. D **62**, 033007 (2000).
[14] G. Barenboim *et al.*, hep-ph/0108199.
[15] G. Barenboim, A.S. Dighe, and S. Skadhauge, Phys. Rev. D **65**, 053001 (2002).
[16] V. Barger *et al.*, Phys. Rev. D **63**, 033002 (2001).
[17] SNO Collaboration, Q.R. Ahmad *et al.*, Phys. Rev. Lett. **89**, 011301 (2002).
[18] V. Barger *et al.*, Phys. Rev. D **58**, 093016 (1998).
[19] Let us see what the effect of a possible violation of adiabaticity between the two highest energy eigenstates, $\overline{\nu}_\mu$ and $\overline{\nu}_\tau$ at high matter densities, in the case of a LSND-inverted (2+2) model [Fig. 1(f)] is on $p_{e\to e}$ and $p_{\mu\to e}+p_{\tau\to e}$. Violation of adiabaticity would result in a non-vanishing hopping probability p_{hop} between these two local Hamiltonian eigenstates. Clearly, $p_{e\to e}$ is unaffected, and also $p_{\mu\to e}+p_{\tau\to e}=p_{hop}|U_{e0}^{evol}|^2+(1-p_{hop})|U_{e1}^{evol}|^2+(1-p_{hop})|U_{e0}^{evol}|^2+p_{hop}|U_{e1}^{evol}|^2=|U_{e0}^{evol}|^2+|U_{e1}^{evol}|^2$ has the same value as in the adiabatic case.
[20] C. Lunardini and A.Y. Smirnov, Nucl. Phys. **B616**, 307 (2001).
[21] M. Koshiba, Phys. Rep. **220**, 229 (1992).
[22] A.Y. Smirnov, D.N. Spergel, and J.N. Bahcall, Phys. Rev. D **49**, 1389 (1994).
[23] KARMEN Collaboration, B. Armbruster *et al.*, Phys. Rev. D **65**, 112001 (2002); K. Eitel (private communication).
[24] Y. Declais *et al.*, Nucl. Phys. **B434**, 503 (1995).
[25] S.M. Bilenky *et al.*, Phys. Rev. D **54**, 1881 (1996); **60**, 073007 (1999).
[26] O.L.G. Peres and A.Y. Smirnov, Nucl. Phys. **B599**, 3 (2001).
[27] J.F. Beacom and P. Vogel, Phys. Rev. D **58**, 053010 (1998); **58**, 093012 (1998); L. Cadonati, F.P. Calaprice, and M.C. Chen, Astropart. Phys. **16**, 361 (2002); P. Vogel, Prog. Part. Nucl. Phys. **48**, 29 (2002); W. Fulgione, Nucl. Phys. B (Proc. Suppl.) **70**, 469 (1999); F. Halzen, J.E. Jacobsen, and E. Zas, Phys. Rev. D **53**, 7359 (1996); M. K. Sharp, J. F. Beacom, and J. A. Formaggio, *ibid.* **66**, 013012 (2002).
[28] B. Jegerlehner, F. Neubig, and G. Raffelt, Phys. Rev. D **54**, 1194 (1996).